

model to explore the effects on electrical stimulation by the ganglion cell body (Finley, 1989). Fig. 19 summarizes the results from this model. The general finding here is that the presence of the cell body, coupled with extracellular electrical field patterns that may be expected in the cochlea, produces significantly different response properties of spatially segmented nodes of Ranvier that appear as polarity- and level-dependent changes of latency and action potential waveshape. As described earlier, Javel's (1989) physiological data tend to support this prediction.

Results obtained with this preliminary model indicate that the presence of the cell body significantly alters the distribution of sites of excitation along the fiber. The effect clearly depends on stimulus polarity and temporal fine structure, and probably on the magnitude and shape of the extracellular potential profile as well. These findings may help explain the bimodal latency distributions of single units to biphasic pulsatile stimuli described by Javel *et al.* (1987) and van den Honert and Stypulkowski (1987), compound action potential waveshapes obtained in response to monophasic stimuli (Stypulkowski and van den Honert, 1984), and extracellularly recorded waveforms of spiral ganglion action potentials (Robertson, 1984).

#### 4. Modeling Studies (White)

Specific aims of work done at UCSF and North Carolina State over the past 7 years have been to account for the stochastic, noisy behavior of the electrically stimulated auditory neuron, and to determine the effects of variable node width and internal resistance on input-output functions and temporal response properties. The models that have been developed to date, and which will be tested and expanded upon in the studies proposed below, are as follows:

**Linear Passive Lumped-Element Neural Model.** In this study, we explored the effects of fiber and node dimensions on excitability. Liberman and Oliver's (1984) findings indicate that a 7:1 range of diameters exists in the cat cochlea for nodes peripheral to the cell body, and that a 3:1 range exists for nodes central to the cell body. In addition, the average node diameter of central nodes is about 3.5 times larger than that for peripheral nodes. In one set of simulations we used a simple passive multi-node model like that illustrated in Fig. 21. The membrane resistance ( $R_m$ ), membrane capacitance ( $C_m$ ), and internal resistance ( $R_i$ ) were estimated for each node using Liberman and Oliver's data on fiber diameters and node dimensions. The analysis showed that, for small diameter cochlear afferents, the axonal resistance ( $R_i$ ) between two adjacent nodes can match or exceed than the transmembrane impedance of the nodes. For small fibers this means that changes in membrane impedance can have a large effect on the voltage developed across the membrane and, therefore, can have a large affect on excitability. In contrast, the voltage developed across nodes in large diameter fibers is relatively insensitive to changing membrane impedance. Because changes in the spectrum of the stimulus change the membrane's impedance, fiber diameter and internode resistance could play an important role in determining a node's sensitivity or insensitivity to such changes.

We determined that the voltage across a node's membrane was directly related to the second spatial derivative of the field in the extracellular medium (Finley *et al.*, 1990). Also, we found that a node's voltage was generally larger if the node was near an abrupt change in impedance (*e.g.*, near a cell-body or near a change in fiber diameter). Because the voltage across a node is a first-order indicator of the node's excitability, the second spatial derivative and impedance discontinuities may be particularly significant variables in determining a node's excitability.

**Nonlinear Deterministic Membrane Model.** We developed a modified Hodgkin-Huxley (H-H) model with a single homogenous node driven with a current source using one internal and one external electrode. Simulations with this model indicate that membrane impedance and excitability can increase dramatically at low sinusoidal frequencies and at low square-wave frequencies (White, 1984; Tasaki, 1982). The behavior appears to be somewhat analogous to a resonant system, where a previous phase of hyperpolarization can increase the membrane's excitability to the next depolarizing phase of stimulation (see Fig. 22). This may explain the extreme dip observed in thresholds at 100 Hz in some fibers (Hartmann and Klinke, 1990) and also observed in behavioral thresholds in patients and animals (Pfungst, 1982). However, Hartmann and Klinke also found fibers that were relatively insensitive to changes in stimulus spectrum. Our simulations of a multi-node passive model (see previous paragraphs) indicate that larger diameter fibers, in contrast to smaller fibers, will be relatively insensitive to changes in membrane impedance due to changes in stimulus spectrum. Thus Hartmann and Klinke's different fiber response profiles may be the result of large differences that exist in fiber diameters in the cochlea.

**Simple Single Node Stochastic Model.** Verveen (1962) postulated that neural membrane noise is generated by individual channel activity in the nodal membrane. In nodes with smaller surface areas there are relatively few channels. Therefore, an individual channel's probabilistic activity has a proportionately greater influence on the node's behavior. Verveen determined how the probability of discharge varies with electrical stimulus intensity for a wide range of fibers with different nodal surface areas. For certain stimulus conditions, Verveen found that functions relating discharge probability to stimulus amplitude were described well by integrated Gaussian



functions. Hill's model (Fig. 23) was modified by Verveen so that it would exhibit this simple form of stochastic behavior (see Fig. 24).

Through a series of experiments Verveen found that the slopes of these fiber input-output functions were monotonically increasing functions of nodal surface area. Using Verveen's equation relating surface area to slope and using measured diameters and lengths of nodes of Ranvier of Type I afferent neurons in the cat cochlea (Liberman and Oliver, 1984), we (White *et al.*, 1987) computed the integrated Gaussian input-output functions for the central (Fig. 25) and peripheral (Fig. 26) processes in the cat. We then computed dynamic ranges in dB for each input-output function by determining the stimulus range required to span an 0.1 to 0.9 response probability for the fiber. The predicted dynamic ranges were nearly identical to those directly measured by Javel *et al.* (1987) in the electrically stimulated cat cochlea. When combined with a commonly used behavioral threshold model, this simple stochastic model has proven useful in predicting behavioral temporal integration functions, psychometric functions, and dynamic ranges from psychophysical experiments (see Preliminary Studies in Project V).

**Spike Latency Model Based on Neural Conduction.** We developed a simple model that predicts spike latency on the basis of estimates of action potential latency through cell segments of variable conduction velocity. In contrast with suggestions (van den Honert and Stypulkowski, 1984) that C responses (Fig. 1) stem from direct excitation of inner hair cells, our model indicates that the time difference between the C and B responses (Fig. 1) may result from an action potential traveling one internodal distance along the very-small-diameter peripheral processes in the cochlea (i.e., 150 microns at approximately 1 meter/sec). The model, if true, suggests that C responses should be observable in recordings from deafened ears.

**Stochastic Multi-Node Model.** In simulations using a simple stochastic multi-node model (Fig. 27), we found that small nodes generated the majority of initial discharges at low stimulus levels. In contrast, this model predicts that larger nodes generate the majority of activity at higher intensities. This behavior was caused by differences in the slopes of input-output functions predicted by excitation at nodes of widely varying diameter. Verveen's (1962) model is also useful at predicting the temporal dispersion or standard deviation of discharge latencies. Specifically, this model predicts that jitter will be relatively large when small nodes are initially excited and will decrease as intensity increases. These predictions are consistent with Javel's data (see Fig. 7) in that the slopes of the input-output functions for the A and B components co-vary with the standard deviations of the latencies in exactly the manner predicted. Also consistent with the model are van den Honert and Stypulkowski's (1984) findings, which indicate that A responses result from excitation of proximal, large diameter nodes.

**Stochastic Multi-Fiber, Multi-Node Model.** Using the same multi-node fiber model, we (White, 1986) studied how neural activity was generated by a representative population of model fibers. Model fibers were constructed to represent the wide range of fiber and node dimensions observed by Liberman and Oliver (1984). At the lowest stimulus levels, the smallest diameter fibers carried the majority of neural activity, with the peripheral nodes initially being excited. At higher stimulus levels, the larger diameter fibers and nodes dominated. As before, this pattern of responses resulted from the differences in the slopes of the input-output functions.

## D. Experimental Design and Methods

### 1. Introduction

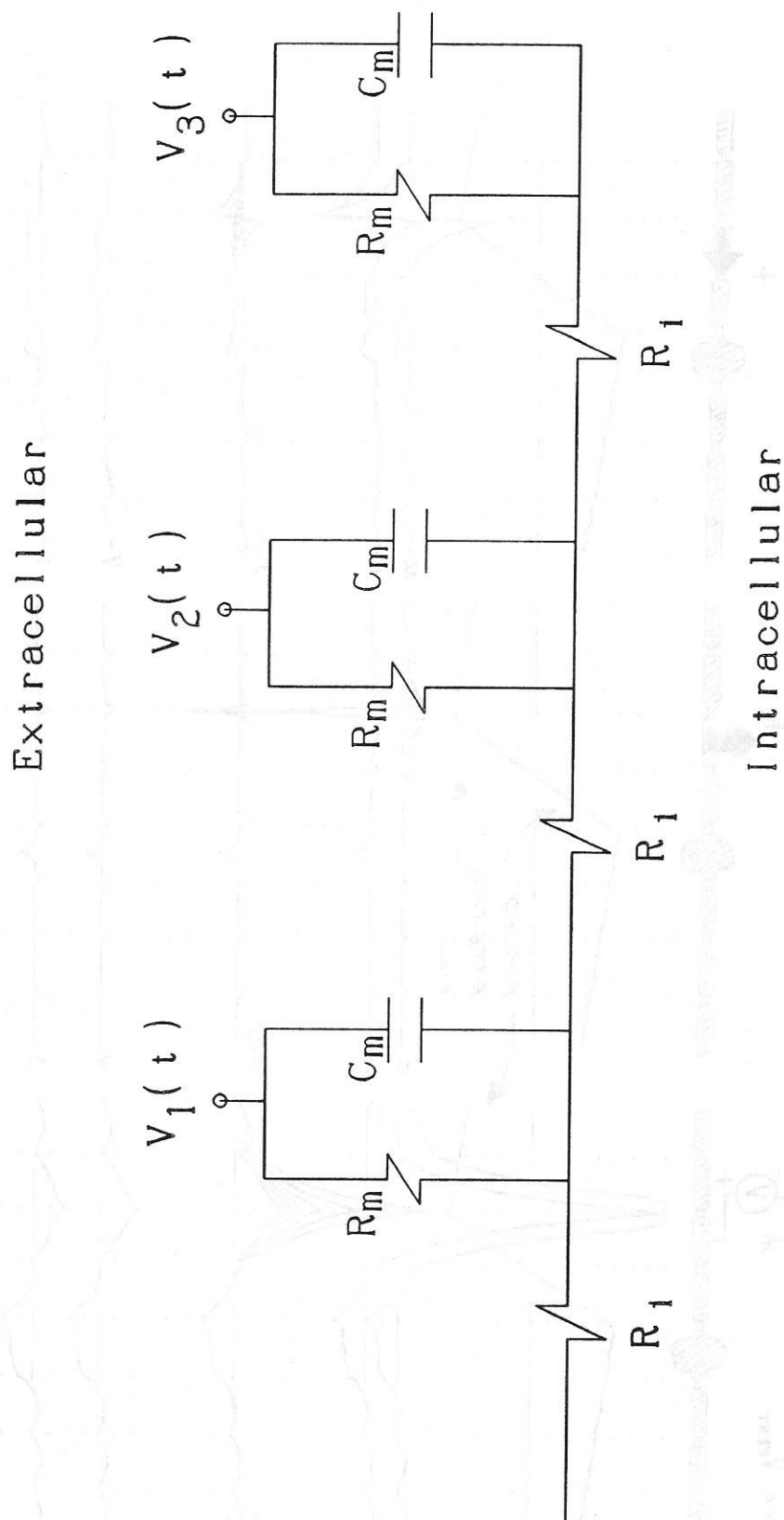
The description of methods provided here involves more detail than is typically presented in Federal grants. It was done this way for a purpose, which was to state all general physiological and histological methods only once in this application, rather than reiterate the same methods in each project. Physiological techniques described in other projects supplement the methods described here and are applicable only to that project.

### 2. General Methods

#### a. Subjects

Single-cell responses of auditory nerve fibers and bushy cells of AVCN will be obtained acutely from young adult cats that exhibit no manifestations of chronic illness or diseases of the external or middle ears. Animals will be purchased from two sources, depending on the way the animal will be studied. Animals used in Projects III and IV will be obtained from the Duke University Division of Laboratory Animal Resources, and animals used in Project V will be obtained from the University of Toronto Research Animal Care Facility. In both cases the animals are purchased from licensed suppliers and housed in the universities' animal care facilities.

Ten cats will be used yearly in Project III, six in Project IV and eight in Project V. Of the animals used in Projects III and IV, approximately half will possess intact hearing prior to implantation, whereas the remainder will be deafened monaurally. Rather than devote an entire experiment to one aspect of a project (e.g., effects of stimulus





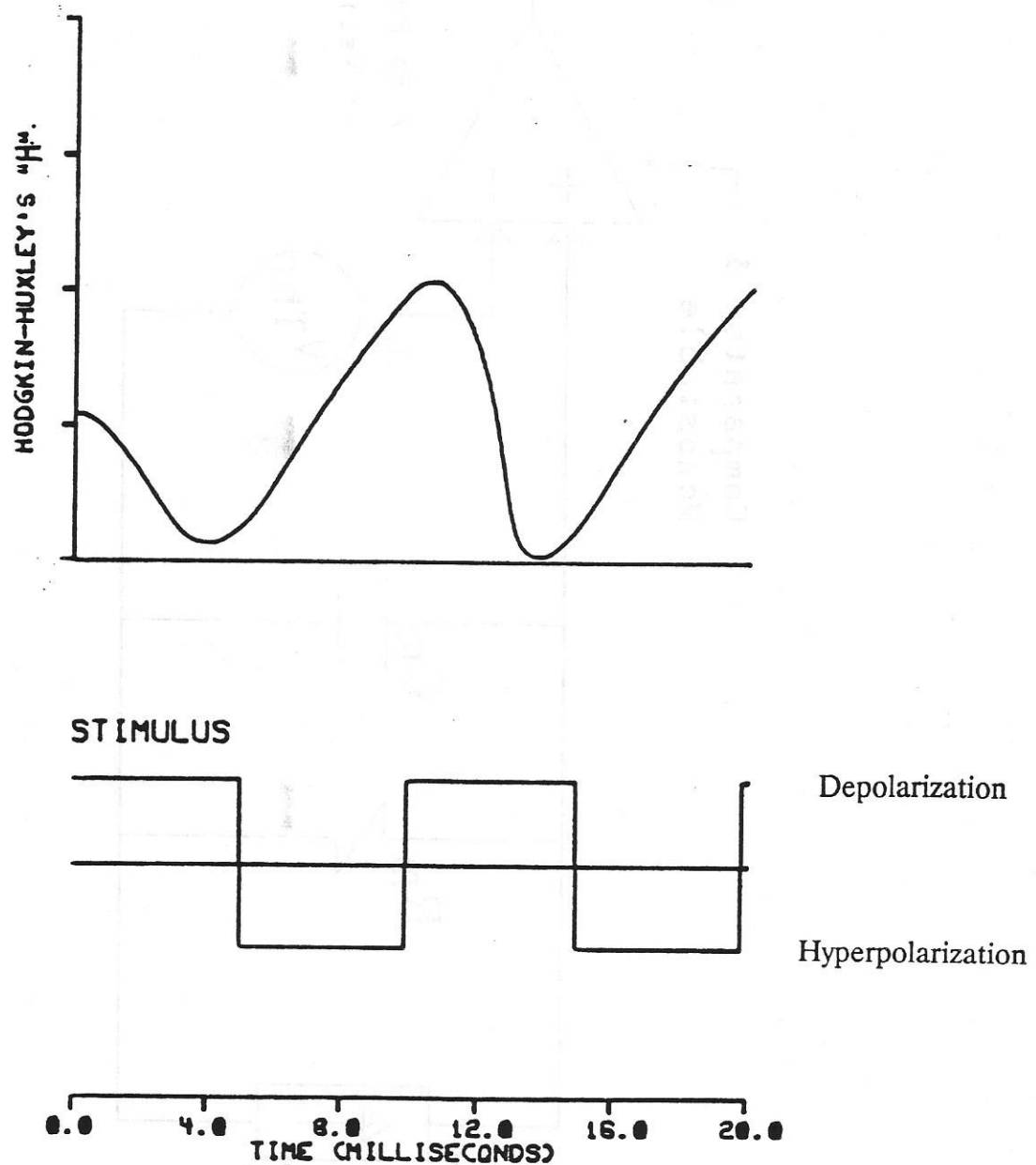


Figure 22 illustrates how " $H$ ," the Hodgkin-Huxley deactivation variable, varies after onset of a 100 Hz square-wave pulse train using a controlled current source. " $H$ " is not very large at the onset of the first depolarizing phase of the stimulus. " $H$ " is greatest after rebounding from the hyperpolarization phase of the stimulus. Because " $H$ " must be relatively large for excitation to occur, this rebound effect appears to improve excitability. Note that the H-H model was modified by increasing beta-h four-fold.

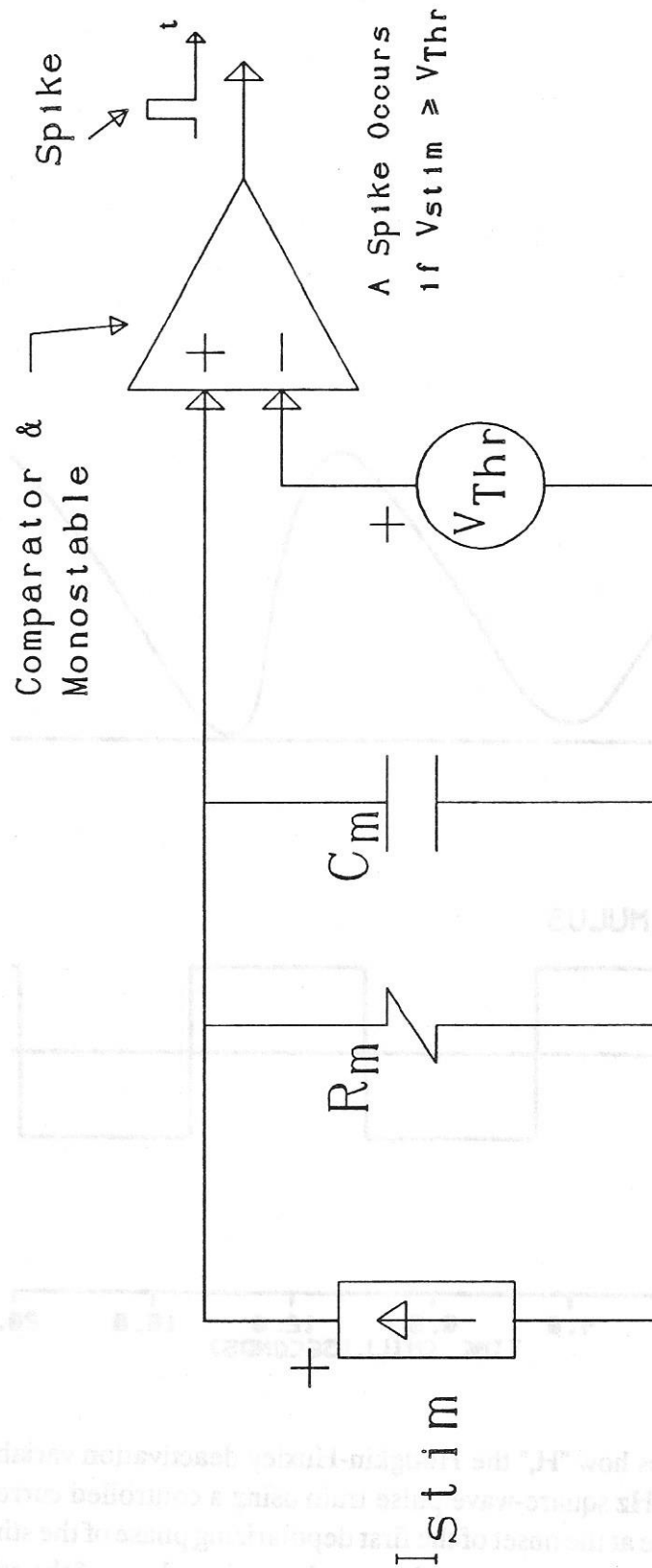
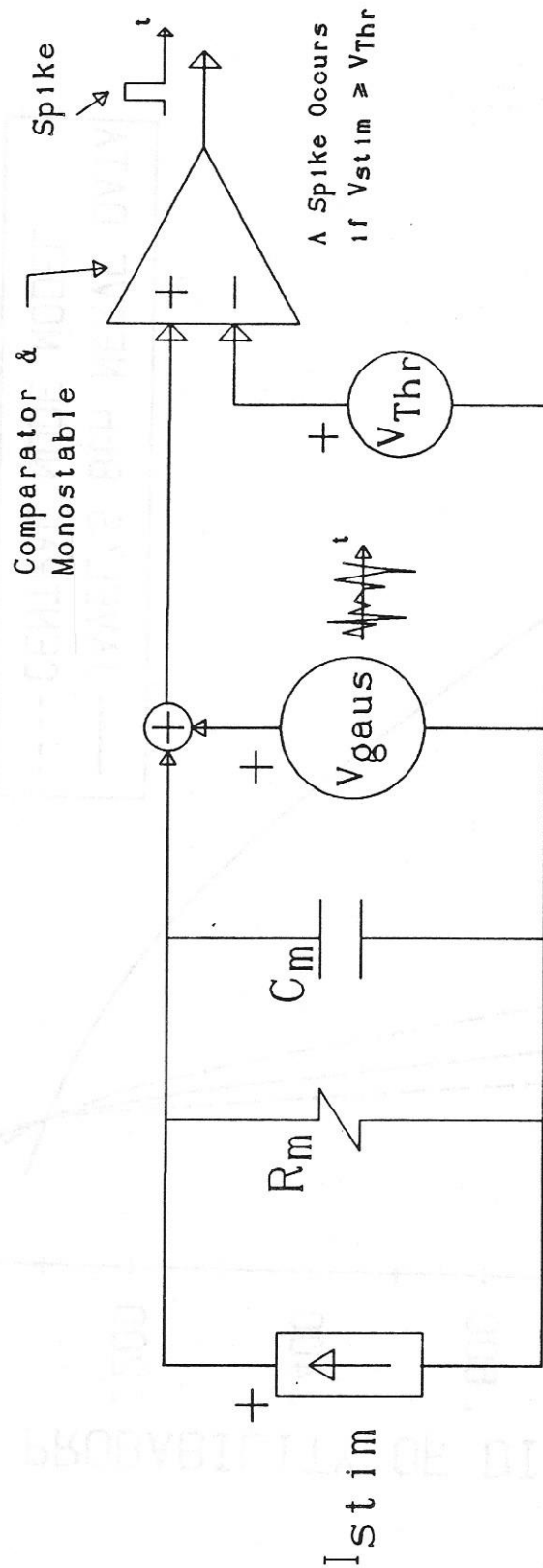


Figure 23. Hill's Model



$V_{gaus}$  is a monotonically decreasing function of the node's surface area.

Figure 24. Hill's Model Modified to Generate Stochastic Behavior.

# 8th NERVE DATA vs CENTRAL NODE MODEL

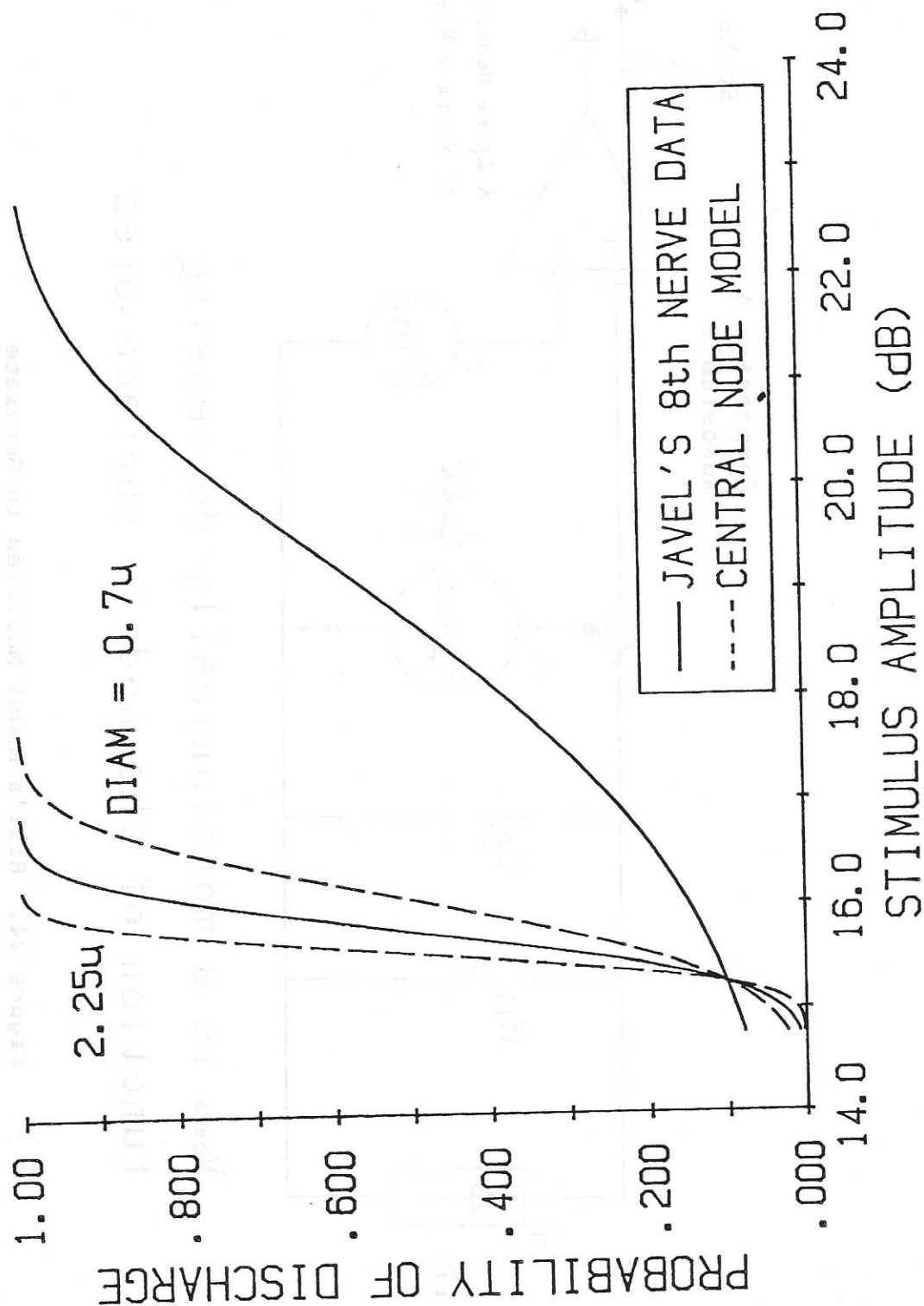


Figure 25. Probability of Discharge vs. Stimulus Amplitude for Central Node Model Compared to Javel's Eighth Nerve Data.

# 8th NERVE DATA vs PERIPHERAL NODE MODEL

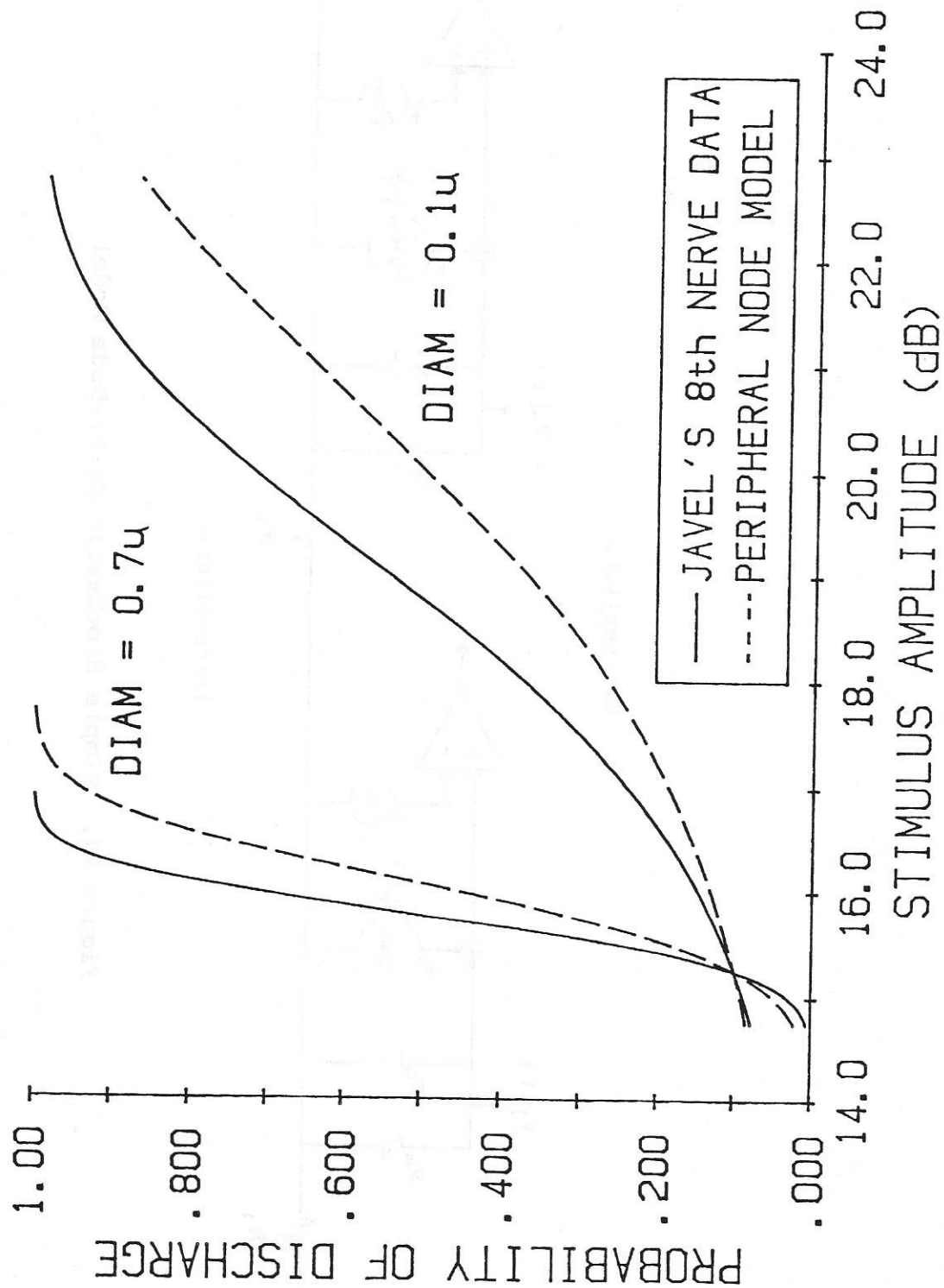


Figure 26. Probability of Discharge vs. Stimulus Amplitude for Peripheral Node Model Compared to Javel's Eighth Nerve Data.



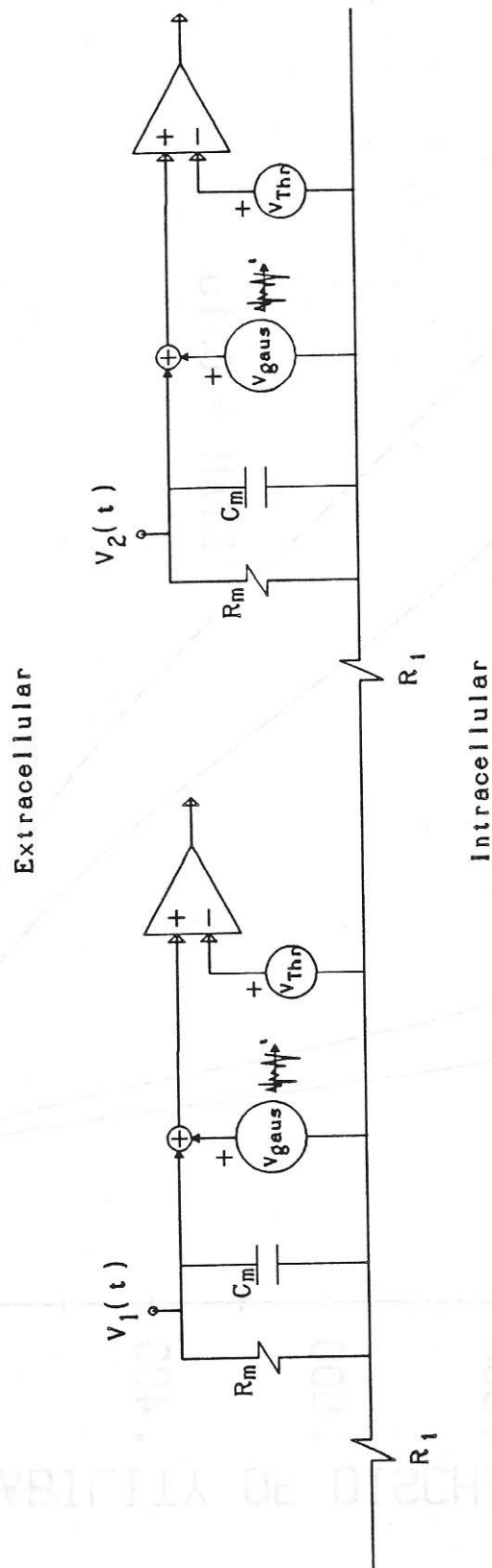


Figure 27. Simple Stochastic Multi-Node Model